Journal of Medical and Biological Engineering (2019) 39:523–531
https://doi.org/10.1007/s40846-018-0433-7

ORIGINAL ARTICLE

Influence of Vitamin D Status and Mechanical Loading on the Morphometric and Mechanical Properties of the Mouse Tibia

Yong-Tao Lu[1,2] · Zhen-Tao Cui[2] · Han-Xing Zhu[3] · Ru-Kun Ma[2] · Cheng-Wei Wu[1,2]

Received: 24 March 2018 / Accepted: 5 June 2018 / Published online: 12 June 2018

Abstract
It is well known that vitamin D and mechanical loading play important roles in bone growth and development. However, the combined effect of the maternal vitamin D status and mechanical loading on the bone quality of growing and mature bones is still unclear. The aim of this study was to investigate the influence of the antenatal vitamin D status and mechanical loading on bone morphometric and mechanical properties in juvenile and adult bones. C57BL/6J mice were used to generate vitamin D-replete and vitamin D-depleted dams. The left tibiae of 8-week-old and 16-week-old offspring were mechanically loaded in vivo for two weeks. Both tibiae were dissected and scanned using a μCT imaging system. It was found that in the bones of 10-week-old juvenile offspring, the antenatal vitamin D-replete group significantly increased trabecular bone volume fraction (Tb.BV/TV), trabecular thickness (Tb.Th), cortical thickness (Ct.Th), bone stiffness and failure load; significantly decreased trabecular separation (Tb.Sp) and cortical marrow area (Ct.MA) only in loaded tibiae; and markedly increased Tb.Sp and Ct.MA only in non-loaded tibiae. In the bones of the 18-week-old adult offspring, the antenatal vitamin D status had a minimal effect on the bone morphometric and mechanical parameters. These data imply that antenatal vitamin D repletion results in increased responses to mechanical loading only in the juvenile state, emphasizing the importance of a sufficient vitamin D supply during pregnancy and sufficient physical activities during the juvenile period to increase bone quality.

Keywords Vitamin D · Mouse tibia · Morphometric analysis · Mechanical properties · Finite element analysis

1 Introduction

Bone is an important component of the human body and plays a crucial role in support and protection to the internal organs of the body. However, abnormally developed bone can lead to an increased risk of bone fracture and an increased chance of developing bone diseases, such as osteoporosis, which is a major skeletal disorder that affects the elderly population [1, 2]. Therefore, to reduce the risk of bone fracture and the occurrence rate of bone diseases, it is crucial to understand the factors that affect the normal growth and development of bone.

It is well known that physical activity and vitamin D are two crucial factors that contribute to the normal growth and development of bone during childhood and are the major measures for maintain bone quality in adult and elderly humans. With respect to the role of physical activity in bone development, previous studies using animal models have shown that external mechanical loading (simulating physical activity) produced higher strains in the bones, which stimulated addition bone formation and consequently increased bone mass [3, 4]. The role of physical activity in bone development can be well explained by the bone mechanoregulation theory, which was first proposed by Frost (1964). Additionally, vitamin D plays a significant role in calcium metabolism and consequently affects bone modeling and remodeling. Numerous clinical and pre-clinical studies have shown that vitamin D level, in later life and also at birth, plays a significant role in bone development [5–7]. For example, a recent study revealed that lower maternal vitamin D status leads to decreased bone mineral contents

✉ Cheng-Wei Wu
cwwu@dlut.edu.cn

[1] State Key Laboratory of Structural Analysis for Industrial Equipment, Dalian University of Technology, No. 2 Linggong Road, Ganjingzi District, Dalian 116024, China

[2] Department of Engineering Mechanics, Dalian University of Technology, Dalian 116024, China

[3] School of Engineering, Cardiff University, Cardiff CF24 3AA, UK

in infants and an increased risk of bone fracture in adulthood [7]. However, previous studies only offer information on the effect of either vitamin D or mechanical loading on bone properties, and no previous studies have investigated the combined effect of maternal vitamin D status and mechanical loading on bone growth and development. In addition, in previous animal studies, only one portion of the whole bone (e.g., tibial proximal region, midshaft) was used [8–10]. Therefore, the effects of mechanical loading and vitamin D status on whole-bone properties are still unknown. Whole-bone properties, and especially mechanical properties (stiffness and strength), are crucial because only the strength of whole bone can be appropriately used to reflect the bone's ability to resist fracture, which is the ultimate goal in applying external bone interventions. However, because the changes in the strength of whole bone due to vitamin D intervention have not been reported thus far, little is known of the associations between local changes in the bone properties and changes in the mechanical properties of the whole bone. This information could reveal the mechanism of how vitamin D and mechanical loading affect bone fracture risk and thus offer important suggestions and strategies for improving bone quality.

The aims of this study were to (1) investigate the influence of antenatal vitamin D status and mechanical loading on the morphometric and mechanical properties of mouse tibia during the periods of continuing skeletal growth (juvenile) and completed skeletal growth (adult) using the techniques of μCT imaging of mouse bone, in vivo mechanical loading, and finite element analysis; and (2) to reveal the associations between the changes in the local bone morphometric properties and the changes in the mechanical properties of whole bone.

2 Materials and Method

2.1 Animals, In vivo Mechanical Loading, μCT Imaging and Image Processing

C57BL/6J mice were used to generate vitamin D-replete and vitamin D-depleted dams. Offspring from the vitamin D-replete and -depleted dams remained on the maternal diet until weaning (Fig. 1), mimicking the common situation of vitamin D exposure in humans. In brief, four-week-old C57BL/6J mice were purchased and housed under the same conditions based on standard procedures. The mice were fed with a vitamin D-supplemented diet (1000 units/kg) or vitamin D-free diet based on the AIN-93G diet (Seebio Biotech Co., Ltd. Shanghai, China) from the age of 4 weeks. At 10 weeks of age, female mice were mated with vitamin D-normal adult males. Dams remained on their respective diets throughout gestation until pup weaning. Offspring (n = 24) remained with their dams until weaning at day 22, at which point they were weaned onto the vitamin D-replete diet. All of the procedures were reviewed and approved by the Local Research Ethics Committee of Dalian University.

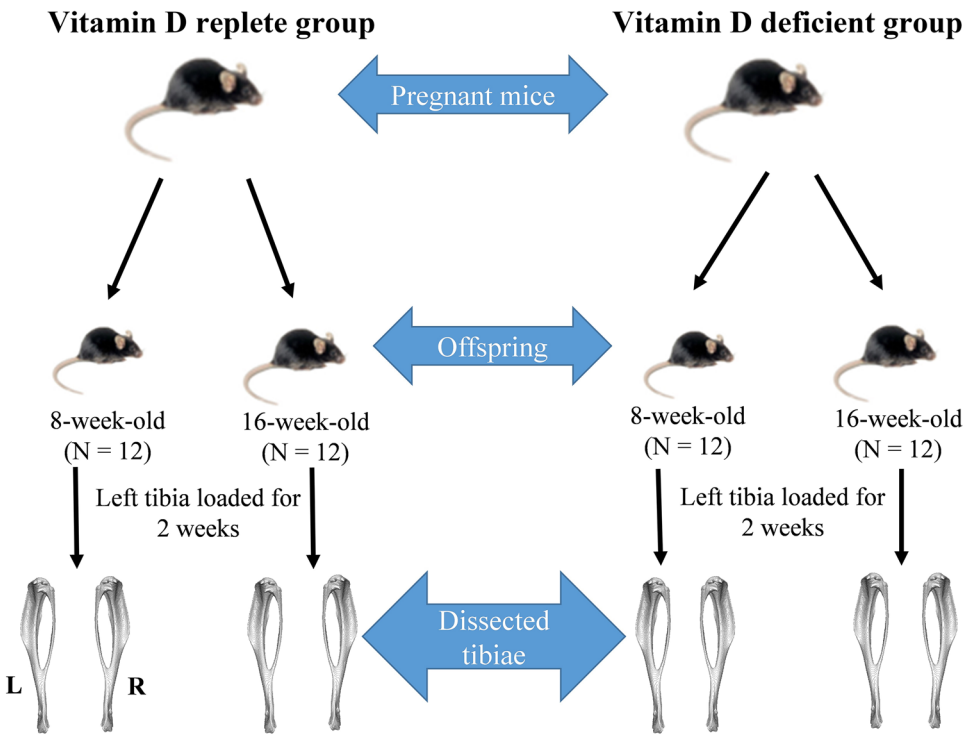

Fig. 1 Experimental design: Offspring of 8-week-old and 16-week-old mice from vitamin D-replete and vitamin D-deficient mother groups were used in investigations. First, the left tibiae were mechanically loaded in vivo for 2 weeks. Second, both tibiae were dissected, and bone morphometric and finite element analyses were performed on both tibiae

A non-invasive method of in vivo tibial loading was used to investigate the bone responses to mechanical loading. The 8-week-old and 16-week-old offspring from both the vitamin D-replete and vitamin D-depleted groups were used in this investigation (Fig. 1). The ages of the mice were chosen to reflect periods of either continuing or completed skeletal growth. Two-week (three times per week) in vivo cyclic compressive loading was performed on the left tibia, which was mounted on an electromechanical universal materials testing machine (MTS Criterion Model 43, MTS Systems Corp., Eden Prairie, Minnesota, USA) with a 100 N load cell, and the contralateral non-loaded limb (right tibia) served as an internal control for mechanical loading. The 10.5 N dynamic load was superimposed onto a 0.5 N preload at a rate of 160000.0 N/s. The in vivo loading protocol consisted of 40 trapezoidal-waveform load cycles (0.2 s hold at 11.0 N) with a 10-s interval between each cycle. The peak load of 11.0 N was selected because this value is known to induce an osteogenic response in female C57BL/6J mice [11, 12]. After mechanical loading, both left and right tibiae were dissected from the 10-week-old and 18-week-old offspring and frozen at − 20.0 °C (Fig. 1). Based on the age of the offspring and the status of mechanical loading, the tibiae were classified into four groups: loaded tibiae from 10-week-old offspring ('10 week + 11 N'), non-loaded tibiae from 10-week-old offspring ('10 week + 0 N'), loaded tibiae from 18-week-old offspring ('18 week + 11 N'), and non-loaded tibiae from 18-week-old offspring ('18 week + 0 N') (Fig. 1). Each group contained 12 mice.

The whole tibia was scanned using an ex vivo μCT imaging system (SkyScan desktop 1172, Bruker, Belgium) at a resolution of 10.4 μm, voltage of 50 kV, tube current of 200 μA, and exposure time of 1180.0 ms. Based on the previously developed image-processing procedure [13, 14], the μCT images were processed using the image processing software Amira (v5.4.3, FEI Visualization Sciences Group, France) prior to morphometric analysis and finite element modeling (Fig. 2). In brief, one left tibia from a 10-week-old offspring was selected as the reference. The long (proximal–distal) axis of the reference tibia was approximately aligned along the z-axis with the y–z plane passing through the central line of the articular surfaces of the medical and lateral condyles (Fig. 2b). To ensure that all of the tibiae were aligned approximately in the same orientation, other left tibiae were aligned to the reference tibia using the method of rigid registration, for which normalized mutual

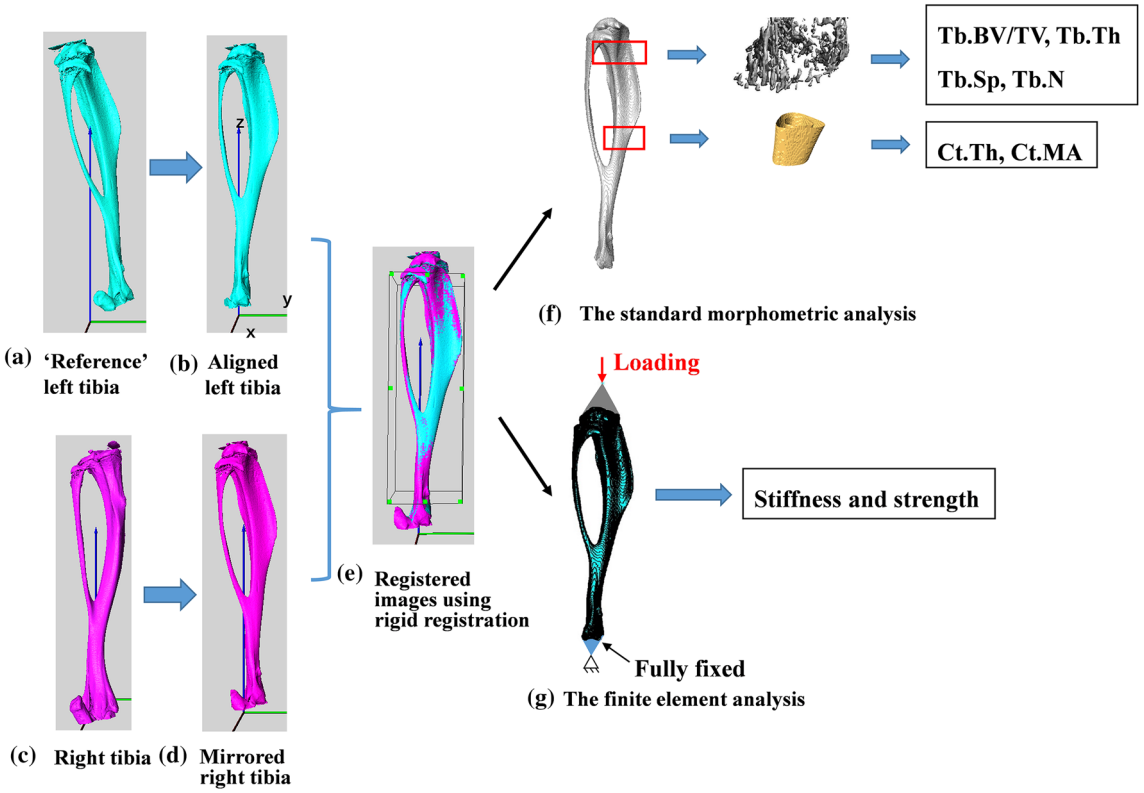

Fig. 2 Schematic procedure for the tibial morphometric and finite element analyses. All of the tibiae were first transformed to the same orientation system. The morphometric analysis was performed on the proximal trabecular portion (trabecular bone volume fraction, thickness, separation and number were calculated) and tibial midshaft (cortex thickness and marrow area were calculated). Finite element analysis was performed on the whole tibia

information was used as an optimization criterion and the Euclidean distance was used as the similarity measure [4]. All of the right tibiae were mirrored first and were subsequently aligned to the reference tibia using rigid registration (Fig. 2d, e). Following registration, the images were transformed to the new positions and resampled using the Lanczos kernel [15].

2.2 Standard Bone Morphometric Analysis

From the resampled μCT images, standard morphometric analyses were performed on the trabecular and cortical bone regions using the procedures developed in the literature [16, 17]. In brief, the grayscale images were first filtered using a Gaussian filter (convolution kernel of $3 \times 3 \times 3$, standard deviation of 0.65) to reduce the high frequency noise [18] and subsequently binarized into bone and background using a fixed single level threshold, which is 25.5% of maximal grayscale value (approximately 420.0 mg HA/cm^3) [19]. For analysis of trabecular bone, a VOI of 1.0 mm in the proximal–distal axis was chosen, starting from the region located 0.2 mm away from the slice where the medial and lateral sides of the growth plate merged (Fig. 2f). From the processed images, the following trabecular morphometric parameters were calculated: trabecular bone volume fraction (Tb.BV/TV), trabecular number (Tb.N), trabecular separation (Tb.Sp) and trabecular thickness (Tb.Th). For analysis of cortical bone, a region of 1.0 mm in the proximal–distal axis in the tibial midshaft was chosen (Fig. 2f), and the following cortex parameters were calculated: cortical thickness (Ct.Th) and cortical marrow area (Ct.MA).

2.3 Finite Element Analysis

Linear elastic and heterogeneous finite element (FE) models of mouse tibiae were generated from the resampled μCT images (Fig. 2g). In brief, the grayscale image datasets were first binarized into bone and background using the procedure for bone morphometric analysis. Because the whole lower limb of mouse was imaged and other bones, such as the femur and foot, were also present in the images, the single threshold method cannot completely isolate the tibia and fibula. Therefore, the tibia and fibula were further manually segmented from other bones using the Amira software. The regions at the tibial-fibula joint and the tibial proximal growth plate were manually filled to allow transmission of loading. After the segmentation, a connectivity filter was used to remove all of the bone islands present in the binary image dataset and retain only the connected tibia-fibula complex. From the filtered binary tibia-fibula images, FE models were created by converting each bone voxel into an eight-node hexahedral element using an Matlab code developed in-house (Matlab 2015a, The Mathworks, Inc. USA) (Fig. 2) [20].

Because different bone voxels have different mineralization levels and because of the presence of the partial volume effect in the images, in the current study, heterogeneous material models were defined in the FE models, and this process was implemented in two steps. First, the bone ash density at each bone image voxel was worked out using the approach of phantom calibration. In the current study, a three-rod phantom with densities of 0, 250 and 750 HA mg/cm^3 was used. The phantom was scanned using the same protocol applied for scanning of the mouse tibia. The relationship between the image grayscale values and the calcium hydroxyapatite (HA)-equivalent BMD were established by working out the image grayscale values at each rod of the phantom. Because the bone ash density was used to calculate the bone modulus, the HA-equivalent BMD was further converted into bone ash density using the relationship established in the literature [21]. In the second step, the Young's modulus (E) for each finite element was calculated from the bone ash density using the exponential density-modulus relationship established in the literature (Eq. 1) [22, 23]. To prevent unrealistic bone modulus values, lower and upper thresholds were set in the density-modulus relationship. A lower bone ash density of 0.4 g/cm^3 was used in the density-modulus relationship because of the presence of hollow regions (such as the tibia-fibula joint and the growth plate) in the μFE bone model. The elastic modulus for the elements with bone ash density less than 0.4 g/cm^3 was set to 0.0104 MPa, which is a value used in modeling of soft tissues [24]. However, certain image voxels might have artificially high grayscale values due to the presence of image noise, which could lead to unrealistically high bone densities. Therefore, an upper threshold value of 1.2 g/cm^3 was defined in the density-modulus relationship to remove the influence of image noise [24]. The values of 0.4 and 1.2 g/cm^3 were chosen because they are the lower and upper limits for bone ash density [21]. In summary, the exponential density-modulus relationship used in the current study was formulated as shown below:

$$E = \begin{cases} 0.0104 & \rho_{\text{ash}} < 400 \\ a \times 10^{-4} \times \rho_{ash}^{b} & 400 \le \rho_{\text{ash}} \le 1200 \\ a \times 10^{-4} \times 1200^{b} & \rho_{\text{ash}} > 1200 \end{cases} \quad (1)$$

where a and b are two constants, $a = 1.127$ and $b = 1.746$ in the current study, E is the Young's modulus (units of GPa) and ρ_{ash} is the bone ash density (units of mg/cm^3).

The heterogeneous FE models were generated by mapping the elastic moduli calculated at each image voxel to the FE meshes using an in-house Matlab code [20]. Poisson's

ratio for all materials was set to 0.3. In total, 96 tibial FE models (12 mice per group) were generated.

The boundary condition applied in the FE models was chosen to mimic the experimental setup used in the in vivo loading of mouse tibia, i.e., uniaxial compression loading. Because the foot-tibia-femur complex was embedded in metal cups in the experimental testing, the loadings were transferred to the tibia-fibula complex through the contact surfaces. Therefore, to mimic the experimental setup, all nodes at the tibial distal surfaces in contact with the mouse foot were coupled to a distal reference point (RP), and all degrees of freedom were fixed at the distal RP. All nodes at the tibial proximal surfaces in contact with mouse femur were rigidly coupled to a proximal RP, and a uniaxial displacement of 1.00 mm was applied at the proximal RP (Fig. 2g). The stiffness and failure load of the mouse tibia were calculated from the FE analysis. The tibial compressive stiffness was calculated as the total reaction forces divided by the displacement of 1.00 mm. The failure load of the mouse tibia was calculated using the maximum principal strain criterion, which was validated in vitro and in vivo in the continuum FE models [25, 26]. In short, the tibial failure load was determined from the histogram plot of principal strains and was the value at which 5% of bone tissues in the region of investigation exceeded the principal strain limits (7300 με as the tensile strain limit and 10,300 με as the compressive strain limit) [25, 27]. In calculating the failure load, Saint–Venant's principle was used to minimize the influence of boundary conditions on the results, and thus the region of investigation was located approximately 2.01 mm (approximately 13.25% of the tibial length) away from the proximal end of the tibia-fibula complex and 1.67 mm (approximately 11.24% of the tibial length) away from the distal end of the tibia-fibula complex.

The models were solved using the FE software Ansys (release 14.0.3, ANSYS, Inc. Cannonsburg, PA, USA) on a workstation (Intel Xeon E-5-2670. 2.60 GHz, 256 GB RAM), and approximately 75 min were required for one FE simulation.

2.4 Statistical Analysis

The differences in bone morphometric properties (Tb.BV/TV, Tb.N, Tb.Sp, Tb·Th, Ct.Th and Ct.MA) and mechanical properties (stiffness and failure load) between the vitamin D-replete and vitamin D-deficient groups and between the mechanically loaded and non-loaded groups were analyzed using the analysis of variance (ANOVA) test. The analysis was performed using SPSS. Data are presented as the mean ± standard deviation (SD) unless otherwise specified, and the probability of type I error was set to 0.05, i.e., $p < 0.05$ was considered statistically significant.

To understand the associations between the adaptations of local bone morphometric parameters and the mechanical properties of whole bone, linear regression analysis was performed. The regression equations and the coefficient of determination (R^2) were computed for the relationships between tibial morphometric and mechanical parameters.

2.5 Results

The influences of antenatal vitamin D status and mechanical loading on bone morphometric parameters are shown in Figs. 3 and 4. For trabecular bone, antenatal vitamin D depletion significantly reduced Tb.BV/TV only in the loaded tibiae of 10-week-old offspring, i.e., in the '10 week + 11 N' group (Fig. 3a) and not in the non-loaded tibiae ('10 week + 0 N' group) or in the tibiae of 18-week-old offspring ('18 week + 11 N' and '18 week + 0 N' groups). Antenatal vitamin D status had a minimal effect on Tb.N, and no significant differences were detected in all four groups (Fig. 3b). The antenatal vitamin D depletion significantly reduced the Tb.Th only in the loaded tibiae of 10-week-old offspring ('10 week + 11 N' group) (Fig. 3c), and no significant differences were found in the other three groups. Antenatal vitamin D depletion significantly increased Tb.Sp in both mechanically loaded and non-loaded tibiae of 10-week-old offspring ('10 week + 11 N' and '10 week + 0 N' groups) (Fig. 3d) and had a minimal effect on Tb.Sp in the tibiae of 18-week-old offspring ('18 week + 11 N' and '18 week + 0 N' groups).

For cortical bone, antenatal vitamin D depletion significantly reduced Ct.Th only in the loaded tibiae of 10-week-old offspring ('10 week + 11 N' group) (Fig. 4a). Antenatal vitamin D depletion significantly increased Ct.MA in both mechanically loaded and non-loaded tibiae of 10-week-old offspring ('10 week + 11 N' and '10 week + 0 N' groups) and in the loaded tibiae of 18-week-old offspring ('18 week + 11 N' group) and had a minimal effect on Ct.MA in the mechanically non-loaded tibiae of 18-week-old offspring ('18 week + 0 N' group) (Fig. 4b).

The influence of antenatal vitamin D status and mechanical loading on bone mechanical parameters is shown in Fig. 5. Antenatal vitamin D depletion significantly reduced tibial stiffness and failure load only in the loaded tibiae of 10-week-old offspring ('10 week + 11 N' group), and had a minimal effect on the FE predicted stiffness and failure load in other three groups ('10 week + 11 N', '18 week + 11 N' and '18 week + 0 N').

The linear correlation analysis between bone morphometric and mechanical parameters is shown in Fig. 6. Because maternal vitamin D status significantly changes the bone morphometric and mechanical properties, primarily in the loaded tibiae of 10-week-old offspring, the correlation analysis was only performed for the data from this group

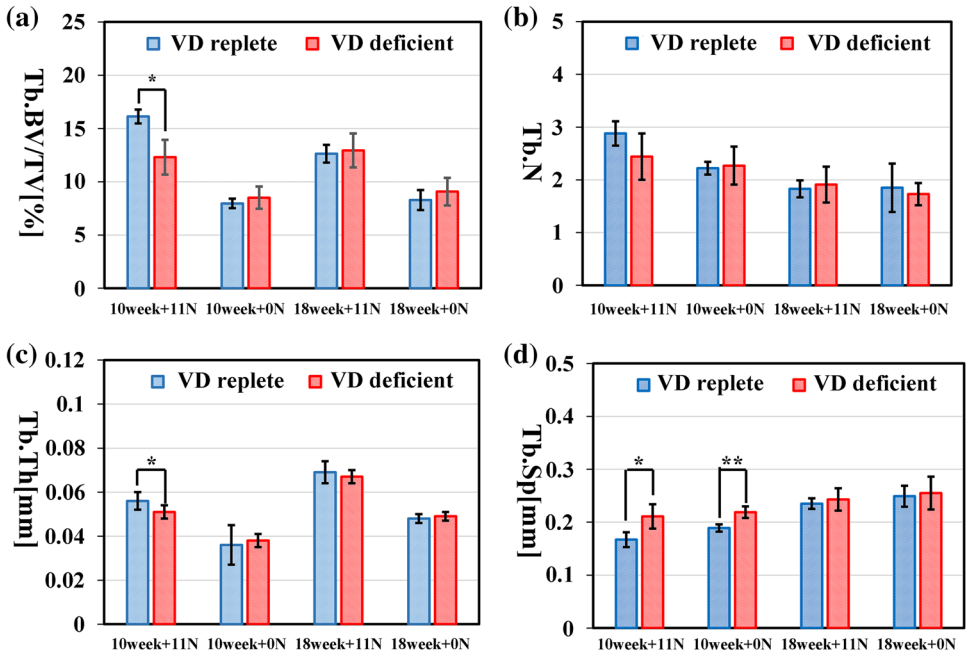

Fig. 3 Combined effect of antenatal vitamin D status and mechanical loading on trabecular bone morphometric parameters (N = 12 per group). Data are presented as the mean values ± standard deviation (*p < 0.05, **p < 0.01)

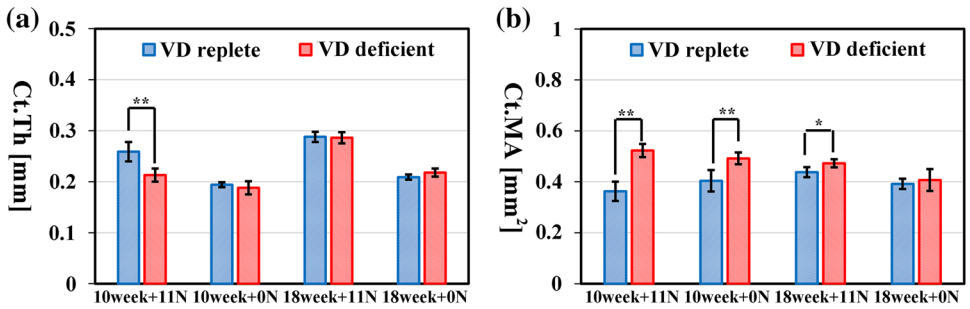

Fig. 4 Combined effect of antenatal vitamin D status and mechanical loading on cortical bone morphometric parameters (N = 12 per group). Data are presented as the mean values ± standard deviation (* p < 0.05, ** p < 0.01)

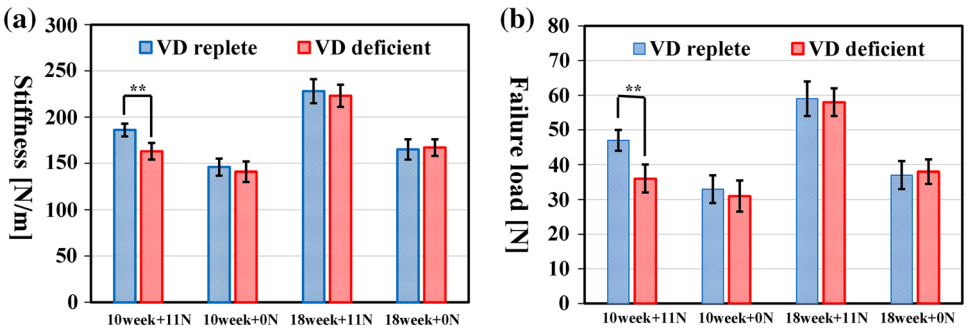

Fig. 5 Combined effect of antenatal vitamin D status and mechanical loading on the mechanical properties of mouse tibia (N = 12 per group). Data are presented as the mean values ± standard deviation (*p < 0.05, **p < 0.01)

('10 week + 11 N' group). Figure 6 shows that the FE predicted tibial failure load was highly linearly correlated with the tibial cortex thickness in both the vitamin D-replete and vitamin D-deficient groups ($R^2 = 0.92$ and 0.89, respectively). The FE-predicted tibial failure load was only mildly linearly correlated with tibial trabecular BV/TV in both the vitamin D-replete and vitamin D-deficient groups ($R^2 = 0.62$ and 0.45, respectively).

3 Discussion and Conclusion

In the current study, the combined effect of antenatal vitamin D status and mechanical loading on the morphometric and mechanical properties of bone in both growing and mature bones was investigated using the techniques of in vivo mechanical loading, μCT imaging and finite element modeling.

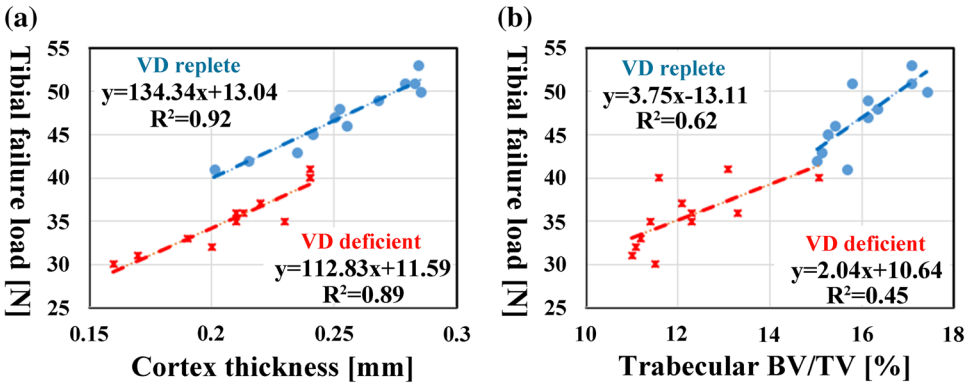

Fig. 6 Linear regression analysis for FE predicted tibial failure load against cortex thickness and trabecular BV/TV for mechanically loaded tibiae of 10-week-old offspring from vitamin D-replete and vitamin D-deficient dams, i.e., data from '10 week + 11 N' groups

Three main findings were revealed in the current study. First, in response to mechanical loading, the effect of antenatal vitamin D status on the bone parameters differs during the period of continuing skeletal growth and during the period of completed skeletal growth. During the period of continuing skeletal growth, in response to mechanical loading, antenatal vitamin D repletion leads to increased Tb.BV/TV, Tb.Th, Ct.Th, bone stiffness and failure load in the loaded tibiae and decreased Tb.Sp and Ct.MA in the loaded tibiae. During the period of completed skeletal growth, only Ct.MA was significantly increased in response to mechanical loading in the loaded tibiae of offspring from antenatal vitamin D-replete dams, which is in agreement with previous studies showing that the aged skeleton is less responsive to mechanical activity [28–30]. However, for the first time, the combined effect of vitamin D status and mechanical loading on bone quality was investigated in juvenile and adult mice in the current study. The data revealed that the mechanical loading that results in bone gain in younger individuals is not able to elicit the same beneficial responses in adult individuals. Such an observation is of general importance to any preventive training concept that aims to maintain bone structure in adult and aged individuals.

Second, the study revealed that the influence of antenatal vitamin D status on bone parameters was different in the mechanically loaded and non-loaded tibiae. In the mechanically loaded tibiae, Tb.BV/TV, Tb.Th, Ct.Th, bone stiffness and failure load were increased in the 10-week-old offspring from antenatal vitamin D-replete dams. In the non-loaded tibiae, antenatal vitamin D status had a minimal influence on bone morphometric and mechanical parameters. The current study is the first to reveal the combined effect of mechanical loading and antenatal vitamin D status on bone parameters, and thus no literature data are available for comparison. The data in the current study imply that vitamin D status alone cannot produce alternations to bone quality. Additional bone appositions were stimulated only after the application of cyclic mechanical loading in the offspring from antenatal vitamin D-replete dams compared with those from the antenatal vitamin D-deficient dams.

Third, the correlation analysis reveals that tibial cortex thickness is highly linearly correlated with tibial failure load and that trabecular BV/TV is only mildly associated with tibial failure load. The explanation for this observation could be that only a small portion of trabecular bone is present in mouse tibia and that the tibial cortex is the main component affected by the mechanical loading. Therefore, changes in the tibial cortex directly lead to the changes in tibial mechanical properties. It should be noted that in the current study, trabecular BV/TV was selected as the representative parameter for trabecular bone because it is a resultant parameter that reflects the changes of other parameters (Tb.N, Tb.Th and Tb.Sp). Additionally, the measurement of Tb.BV/TV is most reliable among all the trabecular morphometric parameters. The finding that the changes in Tb.BV/TV do not necessarily lead to changes in whole-bone mechanical behaviors agrees well with a previous study [16] in which it was also found that it is the total tibial mineral content but not the local trabecular morphometric parameters that is highly associated with the stiffness and failure load of whole bone.

A major novelty in the current study is that state-of-the-art techniques were used to investigate the combined effect of maternal vitamin D, mechanical loading and age on bone properties. For example, the application of in vivo mechanical loading on mouse tibia enables continuous non-invasive external mechanical intervention on the mouse and precise control of external loading parameters, ensuring that the same mechanical loading was applied on each tibia. In addition, the application of the rigid registration technique in the image-processing procedure enables accurate quantifications of bone morphometric and mechanical properties [16]. Another novelty in the current study is that the mechanical behavior of whole bone was characterized using the finite element analysis technique, which is a major advancement over the cross-sectional studies performed in the literature [8–10]. The mechanical strength of whole bone is a key parameter directly linked to bone fracture risk and is therefore crucial to understanding whether the fracture resistance capability of bone is changed by external interventions. However,

both the current study and a recent publication have shown that significant changes in tibial proximal morphometric parameters are not associated with significant changes in the strength of the whole tibia, which implies the importance of investigating whole-bone behavior in addition to the local bone morphometric parameters [16].

Several limitations related to the current study must be noted. First, the combined effects of vitamin D and mechanical loading on bone properties were investigated using animal models and not humans. It could be possible that the mechanisms of bone adaptations regulated by vitamin D and mechanical loading are different in humans and in mice. However, the current study is the first attempt to reveal the combined effect of vitamin D and mechanical loading on bone properties. The next step will be to perform clinical trials to verify the conclusions from the current study. Second, the failure load of the whole bone was predicted from the FE analysis under a relatively simple loading condition, i.e., uniaxial compression loading, and in reality, bone fractures always occur in human femurs and in situations such as a side fall. However, changes in bone adaptations, such as osteoporosis, are systematic, and consequently, reductions of bone strength should occur not only in the femur but also in the tibia and should occur not only under side fall conditions but also under the uniaxial compression condition. Therefore, it is reasonable to take mouse tibia as a representative long bone and uniaxial compression as a representative loading condition for investigating the changes in bone properties caused by external interventions. Finally, only a one-week duration was selected to represent the mouse age period, i.e., 10-week-old mice to represent juvenile status and 18-week-old mice to represent adult status. It is unclear whether an age effect occurs in either the juvenile or adult period. Therefore, in future investigations, additional time points should be selected, but this change requires the sacrifice of many more mice. One solution is to use the state-of-the-art in vivo μCT imaging technique, which enables non-invasive longitudinal monitoring of bone properties [13, 16].

In summary, the current study showed that the influence of antenatal vitamin D status on the bone properties of offspring occurred only on the mechanically loaded bones of growing mice. These data imply that to increase the bone quality (bone stiffness and strength), it is important for the dams to have sufficient vitamin D during pregnancy and for the offspring to perform sufficient physical exercise during childhood.

Acknowledgements This work was funded by the National Natural Science Foundation of China (11702057, 11772086), the Chinese Fundamental Research Funds for the Central Universities (DUT18LK19) and the Open Fund from the State Key Laboratory of Structural Analysis for Industrial Equipment (GZ1611), Dalian University of Technology.

Compliance with Ethical Standards

Conflict of interest The authors declare that there are no financial or personal relationships with other persons or organizations that might inappropriately influence this work.

References

1. Johnell, O., & Kanis, J. (2005). Epidemiology of osteoporotic fractures. *Osteoporos Int, 16*(Suppl 2), S3–S7.
2. Kanis, J. A., & Johnell, O. (2005). Requirements for DXA for the management of osteoporosis in Europe. *Osteoporos Int, 16*(3), 229–238.
3. Levchuk, A., Zwahlen, A., Weigt, C., Lambers, F. M., Badilatti, S. D., Schulte, F. A., et al. (2014). The Clinical Biomechanics Award 2012—presented by the European Society of Biomechanics: large scale simulations of trabecular bone adaptation to loading and treatment. *Clin Biomech, 29*(4), 355–362.
4. Birkhold, A. I., Razi, H., Duda, G. N., Weinkamer, R., Checa, S., & Willie, B. M. (2014). Mineralizing surface is the main target of mechanical stimulation independent of age: 3D dynamic in vivo morphometry. *Bone, 66,* 15–25.
5. Ioannou, C., Javaid, M. K., Mahon, P., Yaqub, M. K., Harvey, N. C., Godfrey, K. M., et al. (2012). The effect of maternal vitamin D concentration on fetal bone. *J Clin Endocrinol Metab, 97*(11), E2070–E2077. https://doi.org/10.1210/jc.2012-2538.
6. Viljakainen, H. T., Saarnio, E., Hytinantti, T., Miettinen, M., Surcel, H., Mäkitie, O., et al. (2010). Maternal vitamin D status determines bone variables in the newborn. *J Clin Endocrinol Metab, 95*(4), 1749–1757.
7. Zhu, K., Whitehouse, A. J., Hart, P. H., Kusel, M., Mountain, J., Lye, S., et al. (2014). Maternal vitamin D status during pregnancy and bone mass in offspring at 20 years of age: a prospective cohort study. *J Bone Miner Res, 29*(5), 1088–1095.
8. Bouxsein, M. L., Myers, K. S., Shultz, K. L., Donahue, L. R., Rosen, C. J., & Beamer, W. G. (2005). Ovariectomy-induced bone loss varies among inbred strains of mice. *J Bone Miner Res, 20*(7), 1085–1092. https://doi.org/10.1359/JBMR.050307.
9. Boyd, S. K., Davison, P., Müller, R., & Gasser, J. A. (2006). Monitoring individual morphological changes over time in ovariectomized rats by in vivo micro-computed tomography. *Bone, 39*(4), 854–862.
10. Klinck, R. J., Campbell, G. M., & Boyd, S. K. (2008). Radiation effects on bone architecture in mice and rats resulting from in vivo micro-computed tomography scanning. *Med Eng Phys, 30*(7), 888–895.
11. De Souza, R. L., Matsuura, M., Eckstein, F., Rawlinson, S. C., Lanyon, L. E., & Pitsillides, A. A. (2005). Non-invasive axial loading of mouse tibiae increases cortical bone formation and modifies trabecular organization: a new model to study cortical and cancellous compartments in a single loaded element. *Bone, 37*(6), 810–818.
12. Willie, B. M., Birkhold, A. I., Razi, H., Thiele, T., Aido, M., Kruck, B., et al. (2013). Diminished response to in vivo mechanical loading in trabecular and not cortical bone in adulthood of female C57BL/6 mice coincides with a reduction in deformation to load. *Bone, 55*(2), 335–346.
13. Lu, Y., Boudiffa, M., Dall'Ara, E., Bellantuono, I., & Viceconti, M. (2016). Development of a protocol to quantify local bone

adaptation over space and time: quantification of reproducibility. *J Biomech, 49*(10), 2095–2099.
14. Lu, Y., Boudiffa, M., Dall'Ara, E., Bellantuono, I., & Viceconti, M. (2015). Evaluation of in vivo measurement errors associated with micro-computed tomography scans by means of the bone surface distance approach. *Med Eng Phys, 37*(11), 1091–1097.
15. Turkowski, K. (1990). Filters for common resampling tasks. In A. S. Glassner (Ed.), *Graphics gems* (Vol. 1, pp. 147–165). Cambridge: Academic Press.
16. Lu, Y., Boudiffa, M., Dall'Ara, E., Bellantuono, I., & Viceconti, M. (2017). Longitudinal effects of parathyroid hormone treatment on morphological, densitometric and mechanical properties of mouse tibia. *J Mech Behav Biomed Mater, 75,* 244–251.
17. Oliviero, S., Lu, Y., Viceconti, M., & Dall'Ara, E. (2017). Effect of integration time on the morphometric, densitometric and mechanical properties of the mouse tibia. *J Biomech, 65,* 203–211.
18. Bouxsein, M. L., Boyd, S. K., Christiansen, B. A., Guldberg, R. E., Jepsen, K. J., & Müller, R. (2010). Guidelines for assessment of bone microstructure in rodents using micro-computed tomography. *J Bone Miner Res, 25*(7), 1468–1486.
19. Klinck, J., & Boyd, S. K. (2008). The magnitude and rate of bone loss in ovariectomized mice differs among inbred strains as determined by longitudinal in vivo micro-computed tomography. *Calcif Tissue Int, 83*(1), 70–79.
20. Chen, Y., Dall Ara, E., Sales, E., Manda, K., Wallace, R., Pankaj, P., et al. (2017). Micro-CT based finite element models of cancellous bone predict accurately displacement once the boundary condition is well replicated: a validation study. *J Mech Behav Biomed Mater, 65,* 644–651.
21. Knowles, N. K., Reeves, J. M., & Ferreira, L. M. (2016). Quantitative computed tomography (QCT) derived bone mineral density (BMD) in finite element studies: a review of the literature. *J Exp Orthop, 3*(1), 36. https://doi.org/10.1186/s40634-016-0072-2.
22. Easley, S. K., Jekir, M. G., Burghardt, A. J., Li, M., & Keaveny, T. M. (2010). Contribution of the intra-specimen variations in tissue mineralization to PTH- and raloxifene-induced changes in stiffness of rat vertebrae. *Bone, 46*(4), 1162–1169. https://doi.org/10.1016/j.bone.2009.12.009.
23. Yang, H., Butz, K. D., Duffy, D., Niebur, G. L., Nauman, E. A., & Main, R. P. (2014). Characterization of cancellous and cortical bone strain in the in vivo mouse tibial loading model using microCT-based finite element analysis. *Bone, 66,* 131–139.
24. Helgason, B., Perilli, E., Schileo, E., Taddei, F., Brynjólfsson, S., & Viceconti, M. (2008). Mathematical relationships between bone density and mechanical properties: a literature review. *Clin Biomech, 23*(2), 135–146.
25. Pistoia, W., van Rietbergen, B., Lochmüller, E. M., Lill, C. A., Eckstein, F., & Rüegsegger, P. (2002). Estimation of distal radius failure load with micro-finite element analysis models based on three-dimensional peripheral quantitative computed tomography images. *Bone, 30*(6), 842–848.
26. Qasim, M., Farinella, G., Zhang, J., Li, X., Yang, L., Eastell, R., et al. (2016). Patient-specific finite element estimated femur strength as a predictor of the risk of hip fracture: the effect of methodological determinants. *Osteoporos Int, 27*(9), 2815–2822.
27. Bayraktar, H. H., Morgan, E. F., Niebur, G. L., Morris, G. E., Wong, E. K., & Keaveny, T. M. (2004). Comparison of the elastic and yield properties of human femoral trabecular and cortical bone tissue. *J Biomech, 37*(1), 27–35.
28. Birkhold, A. I., Razi, H., Duda, G. N., Weinkamer, R., Checa, S., & Willie, B. M. (2014). The influence of age on adaptive bone formation and bone resorption. *Biomaterials, 35*(34), 9290–9301.
29. Holguin, N., Brodt, M. D., Sanchez, M. E., & Silva, M. J. (2014). Aging diminishes lamellar and woven bone formation induced by tibial compression in adult C57BL/6. *Bone, 65,* 83–91.
30. Lynch, M. E., Main, R. P., Xu, Q., Schmicker, T. L., Schaffler, M. B., Wright, T. M., et al. (2011). Tibial compression is anabolic in the adult mouse skeleton despite reduced responsiveness with aging. *Bone, 49*(3), 439–446.